J Wood Sci (2016) 62:276–284
DOI 10.1007/s10086-016-1543-x

ORIGINAL ARTICLE

Effect of thermochemical pretreatment on lignin alteration and cell wall microstructural degradation in *Eucalyptus globulus*: comparison of acid, alkali, and water pretreatments

Kaori Saito[1,5] · Yoshiki Horikawa[2] · Junji Sugiyama[2] · Takashi Watanabe[3] · Yoshinori Kobayashi[4] · Keiji Takabe[1]

Received: 9 December 2015 / Accepted: 1 February 2016 / Published online: 3 March 2016

Abstract Pretreatment is an essential step to effectively hydrolyze lignocellulosic polysaccharides. In this paper, we investigated the degree of decompositions of lignin and cell wall structure using dilute acid, alkali, and water pretreatments to assess both chemical and ultrastructural alterations during pretreatment. The thioacidolysis method showed that β-*O*-4 linkages in lignin were mostly cleaved after all pretreatments, in which the highest decrease of β-*O*-4 units was for NaOH pretreatment, followed by hot water and H_2SO_4 pretreatments. The amounts of lignin degradation compounds, including vanillin and syringaldehyde, in the supernatant water also differed between the three pretreatments. Field-emission scanning electron microscopy revealed clear differences among the pretreatments in decomposing the ultrastructure of the inner surface of the fiber cell walls. Small pores were formed due to degradation of a part of the warty layer of the innermost surface in H_2SO_4 pretreatment. The warty layer was more degraded in hot water pretreatment and thus the cellulose microfibrils of the secondary walls were exposed. NaOH pretreatment showed that the warty layer was almost completely decomposed. The comparative study of different pretreatments using chemical methods and microscopic observations led to a better understanding of decomposition of wood cell walls by thermochemical pretreatment.

Keywords Lignin · Guaiacyl · Syringyl · Secondary cell wall · FE-SEM

Introduction

Woody and herbaceous lignocellulosic plants are increasingly required for the production of ethanol and various bioproducts, because they are widely available as sustainable feedstocks and often not competitive with bioutilized food and feed crops [1, 2]. A major challenge in the bioconversion of plants to ethanol is overcoming the lignocellulose recalcitrance to enzymatic hydrolysis of polysaccharides [3]. Various chemical pretreatment methods for deconstructing the plant cell wall structures have been studied to improve sugar production by enzymatic hydrolysis [4, 5]. However, a comprehensive understanding of both chemical and morphological alterations of plant cell walls by pretreatment is still lacking, which makes the evaluation of factors affecting enzymatic saccharification difficult.

Lignin is the main obstacle to the hydrolysis of polysaccharides. Plant cell walls consist of cellulose microfibrils embedded in an amorphous matrix of lignin

Electronic supplementary material The online version of this article (doi:10.1007/s10086-016-1543-x) contains supplementary material, which is available to authorized users.

✉ Keiji Takabe
kjtakabe@kais.kyoto-u.ac.jp

[1] Laboratory of Tree Cell Biology, Graduate School of Agriculture, Kyoto University, Kyoto 606–8502, Japan

[2] Laboratory of Biomass Morphogenesis and Information, Research Institute for Sustainable Humanosphere, Kyoto University, Uji, Kyoto 611-0011, Japan

[3] Laboratory of Biomass Conversion, Research Institute for Sustainable Humanosphere, Kyoto University, Uji, Kyoto 611-0011, Japan

[4] Japan Bioindustry Association, AIST Tsukuba Central 6, 1-1-1 Higashi, Tsukuba, Ibaraki 305-8566, Japan

[5] Present Address: Laboratory of Biomass Conversion, Research Institute for Sustainable Humanosphere, Kyoto University, Uji, Kyoto 611-0011, Japan

and hemicelluloses through chemical and physical interactions, in which covalent bonds are considered to be present between lignin and hemicelluloses [6, 7]. The difficulty in degrading lignin results from not only interaction with polysaccharides, but also the inherent complexity of the chemical structure. Phenylpropane units with three different methoxy substitutions on the aromatic rings, known as guaiacyl (G), syringyl (S), and *p*-hydroxyphenyl (H) units, are connected via C–O and C–C linkages, including primarily β-*O*-4, β-5, β-β, 5-5, 4-*O*-5, and β-1 types [8, 9]. The resulting lignin macromolecule cannot be isolated in an unmodified form. The relative amounts of G, S, and H units vary between plants species and influence lignin degradability due to differences in the reactivity of each unit [10, 11]. In general, gymnosperm woods (softwood) contain only G units, angiosperm woods (hardwood) have both G and S units, and grasses have additional H units. In the alkaline delignification process of kraft pulping, S units are known to be more readily removed than G units [11, 12].

The degree of alteration of the cell wall microstructures by pretreatment is also important for the enzyme accessibility to cellulose. A plant cell wall is basically subdivided into the middle lamella, primary wall, and secondary wall [13, 14]. Wood has a thickened and lignified secondary wall that contains up to 70–80 % of the total lignin content [15]. The secondary wall further consists of three layers (S_1, S_2, and S_3) having different cellulose microfibril angles [13] (Fig. 1). Pretreatment can reduce physical barriers, including reducing the rigidity of the lignin–polysaccharides network, decreasing cellulose crystallinity, and increasing fiber porosity, thereby exposing the cellulose surface to enzymatic digestion [4, 16]. It has been reported that accessibility of enzymes to the secondary walls in corn stems was enhanced after the removal of lignin, and fungal cellulases penetrated cell walls from the innermost surface through the pore structure of microfibril networks [17]. However, few reports have demonstrated the impact of pretreatment on secondary wall layers.

Pretreatment methods optimal for ethanol production vary with plant species due to their diversity in chemical composition and cell wall structure. The most widely investigated pretreatment techniques include dilute acid [18–20], hot water [21, 22], ammonia fiber expansion [23, 24], and lime [25]. Acid-based and hot water pretreatments affect the solubilization of hemicelluloses rather than lignin, while alkaline pretreatments are mainly effective in extracting of lignin [4, 5, 20, 22]. Pretreatment basically aims to maximize the recovery of available carbohydrates and removal of lignin, but the dissolution of lignin is often disrupted by chemical modifications.

The purpose of this study was to compare the chemical and structural effects of three pretreatments (dilute acid, alkali, and hot water) in *Eucalyptus globulus* and to assess their effects on alterations of lignin and cell wall microstructure. Changes in the lignin chemical structure were evaluated by thioacidolysis, which is a lignin-specific decomposition method used to estimate β-*O*-4 aryl ether-linked units in lignin. Cleavage of the β-*O*-4 units during pretreatment is important for assessing alteration of lignin structure, because the β-*O*-4 bonds are the most abundant and labile linkage types in lignin. We analyzed both residual and solubilized lignin fractions after pretreatment. The alteration of cell wall structures was investigated via submicrometer-scale visualization of fiber cells (Fig. 1), which are the most abundant cell types and provide mechanical support in angiosperm woods. We focused on the innermost cell wall surface of fibers to observe how secondary wall layers are influenced by pretreatments (Fig. 1).

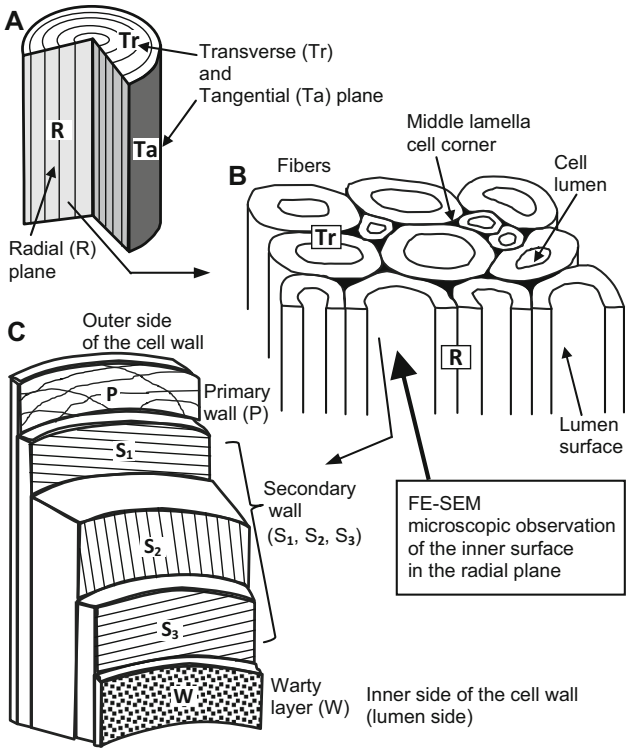

Fig. 1 Schematic diagram of wood structure. **a** A transverse section of wood stem, showing three different directions, transverse (Tr), radial (R), and tangential (Ta) planes; **b** wood fibers arranged longitudinally in which transverse and radial faces are shown. The radial section also shows the innermost surface of the cell walls; **c** multilayered structure of cell walls viewed from the lumen side, illustrating the warty layer (W), the inner (S_3), middle (S_2), outer (S_1) layers of the secondary wall, and the primary wall (P). The different orientations of cellulose microfibrils are shown: the microfibril angle with respect to the fiber axis is 60°–90° in the S_3, 5°–30° in the S_2, and 60°–80° in the S_1 layer of the secondary wall [13]. The primary wall has a multidirectional orientation, and the warty layer has no cellulose microfibrils. In this study, the ultrastructure of the internal surface of fibers exposed in the radial plane was observed by FE-SEM

Materials and methods

Materials

Eucalyptus globulus wood was cut into small blocks and sectioned on a sliding microtome to obtain radial tissue sections (1 cm × 1 cm × 40 μm thick), which were stored in 30 % ethanol and then air-dried before pretreatment.

Pretreatments

Pretreatments were carried out in a Biotage Initiator Sixty microwave using 20 ml reactor vials. The tissue sections (10 mg) were immersed in 20 ml of a water solution (0.05 wt%) containing dilute acid (1.0 % H_2SO_4, v/v), alkali (0.5 % NaOH, v/v), or water. The vials containing a stir bar were sealed and then heated under the following conditions: 5 min at 170 °C for the H_2SO_4 pretreatment, 10 min at 200 °C for the NaOH pretreatment, and 15 min at 200 °C for the water pretreatment. The microwave pretreatment included an initial 1 min heating time to the targeted temperature and 8 min cooling time. The pressure during pretreatments remained under 20 bar. The reaction vessels were cooled to room temperature and centrifuged to separate the pretreated wood residues, followed by washing successively with water. Both the residues and the supernatant solutions were stored at −20 °C until use. In preparation for thioacidolysis, the pretreated residues were air-dried and weighed.

The pH of the supernatant solutions was initially measured as 2 for H_2SO_4, 12 for NaOH, and 5 for hot water. The solutions of NaOH and hot water pretreatments were acidified to pH 3 with dilute HCl. All three supernatant solutions were extracted three times with 30 ml diethyl ether, followed by three times with 30 ml ethyl acetate, and dried with Na_2SO_4. The organic extracts were evaporated to dryness and dissolved in 0.5 ml dichloromethane. The extracts were trimethylsilylated and analyzed by gas chromatography (GC). The peaks were identified and quantified using standard compounds. After GC analysis, ether and ethyl acetate extracts dissolved in dichloromethane were combined and concentrated to dryness under a stream of nitrogen just before thioacidolysis. The experimental protocol is shown in Fig. 2.

For comparison purposes, 21 g of *E. globulus* milled wood samples (100–200 μm diameter) in 700 ml of reaction solvent (3 wt%) was pretreated in an autoclave reactor as previously reported [26]. Pretreatment conditions were almost the same as those with 10 mg wood tissue sections: 5 min at 170 °C for H_2SO_4, 10 min at 210 °C for NaOH, and 15 min at 210 °C for the water pretreatment. The pretreated residues were collected by filtration, washed with water, and stored at −20 °C. The 5 mg residues were air-dried and subjected to thioacidolysis.

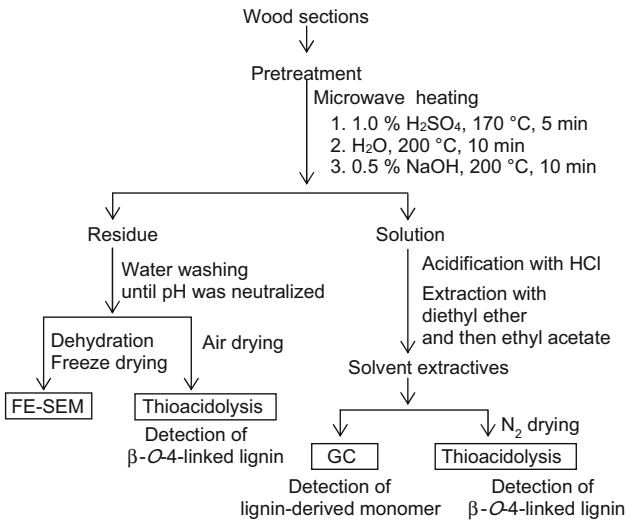

Fig. 2 Analysis of the residual and solubilized fractions obtained after pretreatment

Thioacidolysis

Thioacidolysis was performed on both the residues and organic extracts obtained from the supernatant solution after pretreatment according to a method previously described [27]. Each sample (about 2–5 mg) was added to 5 ml of the thioacidolysis reagent. Thioacidolysis monomeric products were trimethylsilylated and quantified from a GC chromatogram using tetracosane as an internal standard. We used the response factor 1.5 of the main thioacidolysis C6–C3 monomers of the G and S units in GC analysis.

GC

The analysis was conducted with a Shimadzu GC-14A instrument using an HP-1 column (0.25 mm i.d. × 30 m, 0.25 μm film thickness) and flame ionization detector (FID) with He as a carrier gas (1.5 kgf/cm^2). The injector and detector temperatures were set at 250 and 280 °C, respectively. The column temperature program was as follows: for thioacidolysis, 180 °C for 1 min, heated up to 280 °C at 2 °C/min, and held for 10 min, and for the analysis of extracts obtained from supernatant solutions, 80 °C for 1 min, heated up to 280 °C at 5 °C/min, and held for 10 min. Docosane was used as internal standard for quantification of the compounds detected from the supernatant water.

Field-emission scanning electron microscopy (FE-SEM)

The untreated and pretreated tissue sections were dehydrated using a grade series of ethanol solutions (30, 50, 70, 80, 90, and 100 %) and ethanol-*tert*-butanol (1:1) mixture solution, and subsequently freeze-dried using *tert*-butanol. The resulting tissue sections were mounted on carbon double-sided tape attached to aluminum stubs and coated with gold using a Hitachi E-1045 ion sputter (30 mA for 15 s). Microstructures of the radial surface of tissue sections were observed under a FE-SEM (Hitachi S-4800) with an acceleration voltage of 1.5 kV and a working distance of 2.5 mm. A small wood block (1 cm × 1 cm × 1 cm) was also dehydrated, mounted on an aluminum stub, and then coated with gold to obtain the photograph of a clean-cut transverse face under a JEOL JSM-6060 SEM with an acceleration voltage of 5 kV and a working distance of 40 mm.

Results and discussion

Lignin alteration in wood residues after pretreatment

Pretreatments were conducted on thin tissue sections of wood to facilitate FE-SEM observations of cell walls in the pretreated residues. The amounts of thioacidolysis monomeric products as a result of scission of β-*O*-4-linked S and G units of lignin are presented in Table 1. The amounts of β-*O*-4 structures of S and G units after all pretreatments were much smaller compared with the untreated sample (825.6 μmol/g), which suggests that most β-*O*-4 linkages were disrupted during pretreatment. The reduction in β-*O*-4 units was highest in NaOH pretreatment (trace amount), followed by hot water (21.4 μmol/g) and H_2SO_4 pretreatments (55.4 μmol/g). The ratio of S to G units (S:G) decreased after H_2SO_4 pretreatment (78:22 for untreated and 65:35 for H_2SO_4), which indicates that the S units are more readily cleaved than G units during pretreatment, while the S:G ratio did not change significantly during hot water pretreatment (75:25). For NaOH pretreatment, the S:G ratio could not be determined due to the small amounts of thioacidolysis products.

The above thioacidolysis results obtained from mini-scale pretreatment using 10 mg wood tissue sections with 20 ml of reaction solution were compared with those of large-scale pretreatment (Table 1). The large-scale pretreatment reacted 21 g of milled wood with 700 ml of solvent under almost the same pretreatment conditions as the mini-scale pretreatment. For the untreated samples, large-scale pretreatments of the milled wood sample showed a lower yield of the β-*O*-4 structures of both the S and G units (549.7 μmol/g) compared to the tissue section samples used in the mini-scale pretreatment (825.6 μmol/g), although the S:G ratio was almost the same between the milled wood and tissue sections (82:18 and 78:22, respectively). The reason for the lower yield of thioacidolysis monomers in milled wood compared to a tissue section sample is probably due to cleavage of β-*O*-4 linkages during ball milling [28].

For pretreated samples, the large-scale pretreatments showed the similar tendency of the reduction of β-*O*-4 structures compared to the mini-scale pretreatments. The highest reduction was for NaOH, followed by hot water and H_2SO_4 pretreatments. However, the reduction rate was relatively lower for large-scale pretreatments than mini-scale pretreatments, which would be due to differences in the ratio of sample weight to reaction solvent of the large-scale (3 % wood sample in solvent) and the mini-scale (0.05 % wood sample) pretreatments. As shown by the S:G ratio in Table 1, the preferential cleavage of S units over G units in H_2SO_4 mini-scale pretreatment was also observed in H_2SO_4 and NaOH large-scale pretreatments. In contrast, the mini-scale and large-scale hot water pretreatments

Table 1 Yields of S and G thioacidolysis monomers (μmol/g of pretreated woods) obtained after pretreatments at two different scales

Pretreatment	10 mg wood tissue with 20 ml reaction solution					21 g milled wood with 700 ml reaction solution				
	0.05 % (w/v)					3 % (w/v)				
	(μmol/g)					(μmol/g)				
	S	G	S + G	S:G	Preferential decrease	S	G	S + G	S:G	Preferential decrease
Untreated	624.3	183.3	825.6	78:22	–	448.1	101.6	549.7	82:18	–
1.0 % H_2SO_4	36.2	19.2	55.4	65:35	S	74.4	25.6	100.0	74:26	S
Hot water	16.1	5.4	21.4	75:25	S and G	54.2	12.4	66.7	81:19	S and G
0.5 % NaOH	tr	tr	tr	–	S	36.6	14.6	51.2	71:29	S

tr trace

showed no significant difference in the reactivity between S and G units. These differences in the reactivity of S and G units observed in the pretreatments of *E. globulus* were in agreement with previous reports on dilute acid pretreatment of switchgrass [19], alkaline treatment of white birch [11], and hot water pretreatment of *E. globulus* [29]. The *p*-hydroxyphenyl (H) thioacidolysis monomers were not detected in the untreated and pretreated samples. In a previous report, the relative molar abundance of S:G:H monomers detected by thioacidolysis was reported to be 81.3:18.6:0.1 in milled wood lignin isolated from *E. globulus* [9].

The β-*O*-4 linkages are known to be more readily cleaved than other linkages, including 5-5 and β-5 bonds. Several reports have also shown β-*O*-4 cleavage during pretreatments using two-dimensional nuclear magnetic resonance (2D-NMR). A dilute sulfuric acid pretreatment of ball milled lignin from switchgrass resulted in a 36 % decrease in β-*O*-4 linkages at a treatment temperature of 190 °C for 1 min [19]. Steam explosion of aspen wood showed an increased reduction in β-*O*-4 content with increasing severity of the pretreatment condition [30]. Our thioacidolysis results showed a considerable decrease in β-*O*-4 structures (Table 1), which suggests that the network of lignin polymers was substantially altered. One might further expect that lignin is fragmented into the low-molecular-weight segments and released into water. In a previous report [25], however, the chemical composition of the residue pretreated under the same condition as the large-scale pretreatment used here showed that H_2SO_4 and hot water pretreatments gave very little decrease in lignin content and a high reduction in hemicelluloses, whereas NaOH pretreatment led to a relatively high decrease in lignin and a small decrease in hemicelluloses contents. These lignin contents reported were so-called Klason lignin, which is the insoluble residue after H_2SO_4 hydrolysis of polysaccharides. Klason lignin is generally accepted as a standard method, but in some cases overestimated because of possible contamination of proteins and other compounds [31]. The Klason lignin content after dilute acid pretreatments was pointed out to be overestimated because sugar degradation products and other low-molecular-weight compounds were repolymerized through pretreatment [32]. In this report, we analyzed the lignin fraction solubilized in the supernatant water to examine the amount of lignin degradation compounds released from wood after pretreatment.

Solubilized lignin fraction after pretreatment

The lignin fraction solubilized into the supernatant water solution after pretreatment can contain monomers, dimers, and possibly oligomers. These lignin-derived compounds were solvent-extracted, and then not only analyzed by GC, but also subjected to thioacidolysis to detect the β-*O*-4 linkages remaining in the supernatant fraction. Table 2 summarizes the results of the molar contents of the thioacidolysis monomers and lignin monomers [syringaldehyde (Sa), vanillin (Va)] detected from both the residues and supernatant solution after mini-scale pretreatment. Table 2 also presents data on the loss of sample weight after pretreatment. Note that the molar amounts of monomers were calculated per the wood residue or the solubilized wood. This allows us to estimate the percentage of monomers detected in the residue and supernatant against the β-*O*-4 structures obtained from the untreated wood, when we consider that the monomers are derived from the β-*O*-4-linked units (Figure S1). In fact, the monomers remaining in the residue after the H_2SO_4 and hot water pretreatments were 4.1 and 1.2 %, respectively, of those in the untreated wood (Table 2).

GC analysis showed that Sa and Va were the most abundant compounds in supernatant water (Figure S2). Other peaks detected by GC were not identified. As shown in Table 2, the amounts of Sa and Va were highest in the NaOH pretreatment, followed by hot water and H_2SO_4, which is consistent with the descending order of the reduction in β-*O*-4 units found in the pretreated residues. For NaOH pretreatment, the molar amounts of Sa and Va were 1.23 and 0.28 μmol, respectively, or 0.22 mg for Sa and 0.04 mg for Va from 10 mg of the wood sample, corresponding to about 18 % of the β-*O*-4 units detected in untreated wood (8.25 μmol). In contrast, the sums of Sa and Va detected from H_2SO_4 and hot water pretreatments were estimated to be only 1.4 and 4.6 %, respectively, of the β-*O*-4 units of the untreated samples. The Sa:Va ratio was close to or higher than the S:G ratio of the untreated samples for all three pretreatments, regardless of the differences in the cleavage reactivity between the S and G units observed in the pretreated residue. This suggests that the production of Sa is more stable than Va during pretreatments.

The solubilized lignin fraction was further analyzed by thioacidolysis to detect β-*O*-4 units retaining the phenylpropane C6–C3 side chain. The main thioacidolysis monomeric product (i.e., the erythro/threo trithioethylated C6–C3 monomers) is reported to be detected from not only the polymer structure having β-*O*-4 linkages, but also β-*O*-4 dimer model compounds [33]. The thioacidolysis results in Table 2 show that the β-*O*-4 units of S and G units were most predominant in hot water (0.24 μmol) and much lower in H_2SO_4 and NaOH pretreatments (0.02 and 0.02 μmol, respectively). The S:G ratio of the β-*O*-4 structures was kept almost constant during hot water pretreatment compared to the untreated wood (72:28 and 78:22, respectively), while H_2SO_4 and NaOH

Table 2 Yields of thioacidolysis monomers and lignin monomers [syringaldehyde (Sa) and vanillin (Va)] in the residual and solubilized fractions after pretreatment

Pretreatment	Residue					Solubilized fraction into supernatant water									
	Weight (mg)	Thioacidolysis monomers (μmol)				Weight[a] (mg)	Lignin monomers (μmol)				Thioacidolysis monomers (μmol)				Yields[b] of monomers in the supernatant (%)
		S	G	S + G	S:G		Sa	Va	Sa + Va	Sa:Va	S	G	S + G	S:G	
Untreated		6.42	1.83	8.25	78:22										
1.0 % H_2SO_4	6.1	0.22	0.12	0.34	65:35	3.9	0.09	0.02	0.11	83:17	0.02	nd	0.02	100:0	1.7
Hot water	4.5	0.07	0.02	0.10	75:25	5.6	0.32	0.06	0.38	85:15	0.16	0.06	0.24	72:28	7.2
0.5 % NaOH	3.6	tr	tr	tr	–	6.4	1.23	0.28	1.51	81:19	0.01	tr	0.02	90:10	18.5

Yields of thioacidolysis monomers and Sa and Va are expressed as μmol per residual or solubilized wood (per each weight)

tr trace, *nd* not detected

[a] Weight of solubilized fraction was calculated from subtracting the weight of residual wood from the initial weight (i.e., 10 mg)

[b] The yield of the sum of (Sa + Va) + (S + G) in the solubilized fraction and its percentage against the amounts of the thioacidolysis monomers recovered from the untreated wood (8.25 μmol)

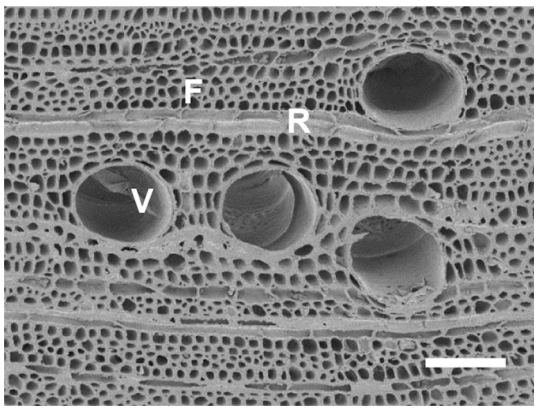

Fig. 3 Transverse surface of *E. globulus* observed under a SEM. The wood is build up mainly of fibers (F) and vessel elements (V). Ray parenchyma cells (R) run in the radial direction. *Scale bar* 100 μm

pretreatments provided few G units with β-*O*-4 linkages. The relatively higher content of β-*O*-4 units and the unaltered S:G ratio in the hot water-treated supernatant fraction suggests the decomposition of lignin with relatively smaller modifications compared to the H_2SO_4 and NaOH pretreatments. The molar amounts of the sum of monomers (Sa and Va) and the β-*O*-4 units in the supernatant water accounted for 1.7 % for H_2SO_4, 7.2 % for hot water, and 18 % for NaOH pretreatments compared to the molar contents of the β-*O*-4 units in untreated wood. These results shows that the three pretreatments differed in the amounts of lignin degradation compounds released into water, in which the highest release was for NaOH pretreatment, followed by hot water and H_2SO_4 pretreatments.

Alteration of the cell wall ultrastructure after pretreatment

The degree of cell wall alteration of the wood residue after pretreatment was evaluated by visualizing the innermost surface of the fiber cell walls (Fig. 1). Because the innermost surface is easily accessible by reaction reagents during pretreatment, the pretreatment effect on the cell wall morphology is clearly assessed. The structure of *E. globulus* before pretreatment is shown in Fig. 3. *E. globulus* is a diffuse-porous wood, in which vessels are surrounded by the fibers (Figure S3).

Figure 4 shows FE-SEM images of the fiber cell walls of the untreated and pretreated radial sections. The cell wall alterations between pretreatments were compared using different magnifications of FE-SEM images. The photograph obtained with 500-fold magnification in the untreated wood (Fig. 4a) shows the several fibers in which their innermost surfaces are observable by cutting along the fiber axis in the radial section. The specimens pretreated

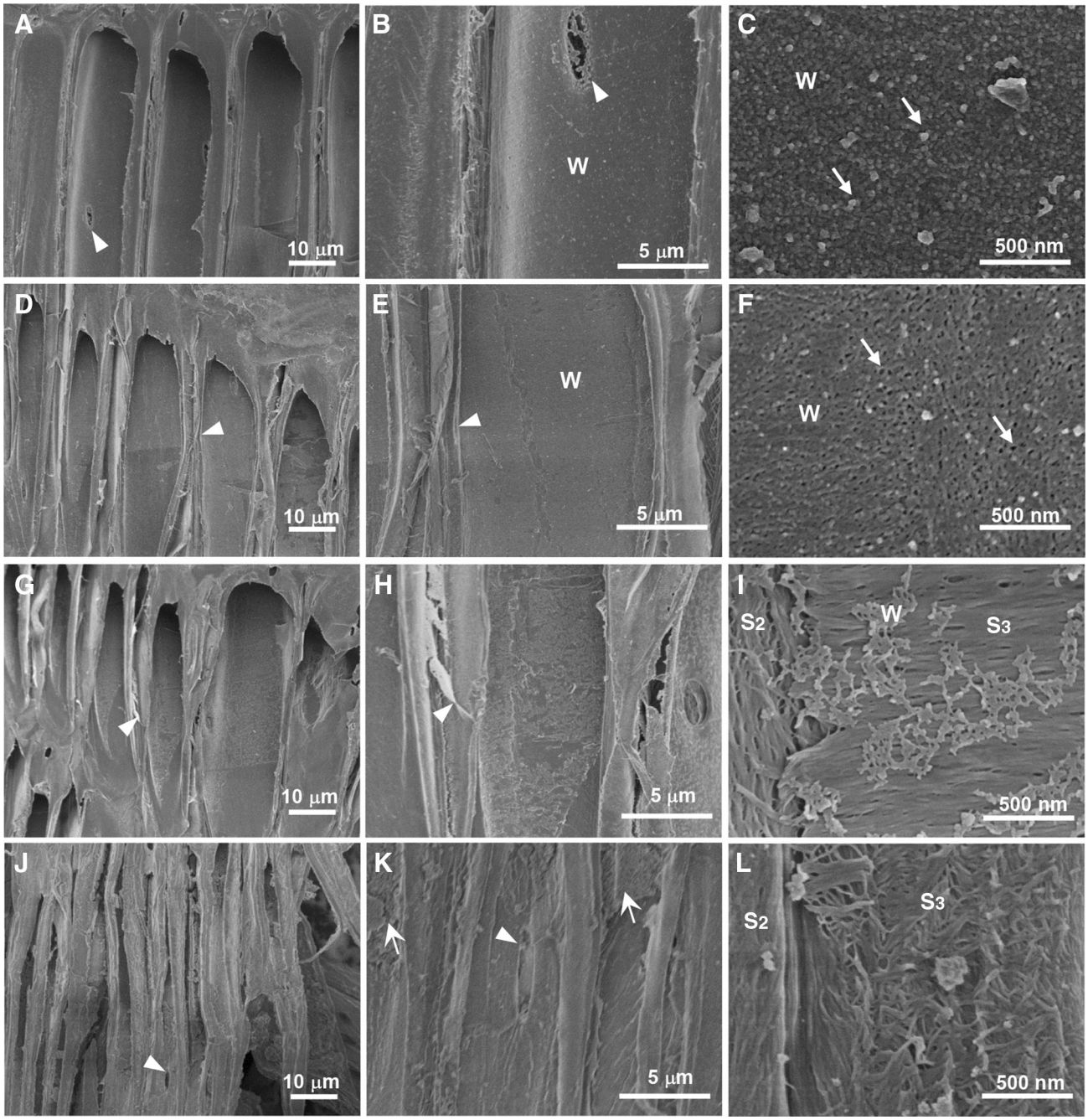

Fig. 4 FE-SEM images of fibers without pretreatment (**a**–**c**) and after pretreatment of H_2SO_4 (**d**–**f**), hot water (**g**–**i**), and NaOH (j–**l**). The photographs are obtained at magnifications of 500 (**a**, **d**, **g**, **j**; *scale bar* 10 μm), 5000 (**b**, **e**, **h**, **k**; *scale bar* 5 μm), and 50,000 (**c**, **f**, **i**, **l**; *scale bar* 500 nm), in which the warty layer (W) and the S_3 and S_2 layers of secondary wall are also shown. The same position is marked by *arrowheads* for each different pretreatment condition (**a** and **b**, **d** and **e**, **g** and **h**, **j** and **k**). *Arrows* in **c**, **f** show small globular structures and small pores present in the warty layer, respectively. *Arrows* in **k** indicates unknown substances deposited on the internal surfaces of fibers

with H_2SO_4 and hot water (Fig. 4d, g, respectively) showed that the fibers tended to detach from the adjacent fibers. The NaOH-pretreated fibers were more severely altered (Fig. 4j). They were slightly or entirely separated from each other and seemed to roll toward the lumen.

The micro- and submicron-scale structures of the fiber lumen were assessed with higher magnification images of 5000- and 50,000-fold, respectively. The innermost surface of the untreated fibers has a warty layer in which the small globular structures are densely distributed, thus the fibrous

structure is not apparent (Fig. 4c). The warty layer covering the secondary wall does not contain cellulose and is considered to be mostly composed of lignin (or lignin-like compounds) and hemicelluloses such as xylan [34–36]. The inner surface of *E. globulus* did not exhibit a distinctly larger wart structure. The image of H_2SO_4 pretreatment depicted the relatively rough surface of the lumen side compared to untreated fibers (Fig. 4e). The image of the rough surface at the submicron level revealed that many small pores (approximately 10 nm or larger size) were distributed almost uniformly, and the globular structures decreased substantially (Fig. 4f). This indicates that part of the warty layer was degraded by H_2SO_4 pretreatment.

Hot water pretreatment (Fig. 4h) shows an inner surface with higher roughness compared to surfaces obtained after H_2SO_4 pretreatment, which is more clearly explained from the submicron-scale image (Fig. 4i). The warty layer was considerably decomposed and peeled off, and the fibrous structures of the S_3 layer and part of the S_2 layer were visible. The cellulose microfibrils of the S_2 layer are oriented almost parallel to the fiber axis, whereas the S_3 layer has an average microfibril angle of 60°–90° (see Fig. 1). For NaOH pretreatment (Fig. 4k), the fibers were most severely modified among the three pretreatments, and unexpectedly, considerable amounts of aggregated unknown substances were heterogeneously deposited on and partly covered the inner surface (Figure S4). At the submicron level, a warty layer was not visibly confirmed, the microfibrils of the S_3 layer were swollen and wavy, and the S_2 layers were partially observed (Fig. 4l). Alkaline pretreatment is known to cause swelling of the cell walls [4, 5]. The waving behavior of the cellulose microfibrils of the S_3 layer has been observed in *Fagus crenata* fibers after delignification following xylanase treatment [34].

We now discuss the results of lignin and cell wall structural alterations. First, H_2SO_4 pretreatment had the lowest reduction of the β-*O*-4 units of lignin. FE-SEM showed that only part of the warty layer was decomposed, which may resulted from the removal of mostly hemicelluloses and partially lignin. However, many small pores formed on the inner surface may impact on the accessibility of hydrolytic enzymes to cellulosic substrate. Second, hot water pretreatment showed the higher reduction of the β-*O*-4 units and more degraded cell wall structures than H_2SO_4 pretreatment. The warty layer was extensively removed, and thus the secondary wall layers were apparent. Finally, NaOH pretreatment with the highest reduction of the β-*O*-4 units showed that the warty layer was almost entirely removed and the swelled cellulose microfibrils of the secondary walls were exposed. The enzymes may be accessible to cellulose, but the water-insoluble deposits on the surface of cellulose microfibrils might prevent the enzyme access in NaOH pretreatment. Further study of enzymatic digestion is needed to better understand the results of the pretreatment effect on both lignin and cell wall microstructural alterations presented in this study.

Conclusion

The alterations of lignin and cell wall structures following different pretreatments were investigated using chemical and microscopic techniques. The main results are summarized as follows:

1. The reduction in β-*O*-4 linkages was highest in NaOH pretreatment, followed by hot water and H_2SO_4 pretreatments. While H_2SO_4 and NaOH pretreatments resulted in a decrease in the S:G ratio, the S:G ratio was kept almost constant during hot water pretreatment.
2. The amounts of lignin degradation products, which include vanillin and syringaldehyde, detected in the supernatant water were highest in the NaOH pretreatment, followed by hot water and H_2SO_4 pretreatments.
3. The alterations of the structures of fiber cell walls differed between the three pretreatments. The degree of decomposition of the inner surface structure of the fibers was highest in the NaOH pretreatment, followed by hot water and H_2SO_4 pretreatments.

Acknowledgments This work was supported by the New Energy and Industrial Technology Development Organization (NEDO). We are grateful to Hoang Nguyen Viet Hoa for her help in SEM measurement.

References

1. Yuan JS, Tiller KH, Al-Ahmad H, Stewart NR, Stewart CN Jr (2008) Plants to power: bioenergy to fuel the future. Trends Plant Sci 13:421–429
2. Ragauskas AJ, Beckham GT, Biddy MJ, Chandra R, Chen F, Davis MF, Davison BH, Dixon RA, Gilna P, Keller M, Langan P, Naskar AK, Saddler JK, Tschaplinski TJ, Tuskan GA, Wyman CE (2014) Lignin valorization: improving lignin processing in the biorefinery. Science 344:1246843
3. Himmel ME, Ding SY, Johnson DK, Adney WS, Nimlos MR, Brady JW, Foust TD (2007) Biomass recalcitrance: engineering plants and enzymes for biofuels production. Science 315:804–807
4. Kumar P, Barrett DM, Delwiche MJ, Stroeve P (2009) Methods for pretreatment of lignocellulosic biomass for efficient hydrolysis and biofuel production. Ind Eng Chem Res 48:3713–3729
5. Alvira P, Tomas-Pejo E, Ballesteros M, Negro MJ (2010) Pretreatment technologies for an efficient bioethanol production process based on enzymatic hydrolysis: a review. Bioresour Technol 101:4851–4861
6. Watanabe T, Ohnishi J, Yamasaki Y, Kaizu S, Koshijima T (1989) Binding-site analysis of the ether linkages between lignin and hemicelluloses in lignin-carbohydrate complexes by DDQ-oxidation. Agric Biol Chem 53:2233–2252

7. Balakshin M, Capanema E, Gracz H, Chang HM, Jameel H (2011) Quantification of lignin–carbohydrate linkages with high-resolution NMR spectroscopy. Planta 233:1097–1110
8. Ralph J (2010) Hydroxycinnamates in lignification. Phytochem Rev 9:65–83
9. Rencoret J, Gutiérrez A, Nieto L, Jiménez-Barbero J, Faulds CB, Kim H, Ralph J, Martínez AT, Del Río JC (2011) Lignin composition and structure in young versus adult *Eucalyptus globulus* plants. Plant Physiol 155:667–682
10. Chang H, Sarkanen KV (1973) Specis variation in lignin-effect of species on rate of kraft delignification. Tappi 56:132–134
11. Tsutsumi Y, Kondo R, Sakai K (1995) The difference of reactivity between syringyl lignin and guaiacyl lignin in alkaline systems. Holzforschung 49:423–428
12. Shimizu S, Yokoyama T, Akiyama T, Matsumoto Y (2012) Reactivity of lignin with different composition of aromatic syringyl/guaiacyl structures and erythro/threo side chain structures in β-*O*-4 type during alkaline delignification: as a basis for the different degradability of hardwood and softwood lignin. J Agric Food Chem 60:6471–6476
13. Plomion C, Leprovost G, Stokes A (2001) Wood formation in trees. Plant Physiol 127:1513–1523
14. Sjöström E (1993) Wood chemistry. Fundamentals and applications, 2nd edn. Academic Press, San Diego, pp 1–20
15. Fergus BJ, Procter AR, Scott JAN, Goring DAI (1969) The distribution of lignin in sprucewood as determined by ultraviolet microscopy. Wood Sci Technol 3:117–138
16. Cheng G, Varanasi P, Li C, Liu H, Melnichenko YB, Simmons BA, Kent MS, Singh S (2011) Transition of cellulose crystalline structure and surface morphology of biomass as a function of ionic liquid pretreatment and its relation to enzymatic hydrolysis. Biomacromolecules 12:933–941
17. Ding SY, Liu YS, Zeng Y, Himmel ME, Baker JO, Bayer EA (2012) How does plant cell wall nanoscale architecture correlate with enzymatic digestibility? Science 338:1055–1060
18. Samuel R, Pu Y, Raman B, Ragauskas AJ (2010) Structural characterization and comparison of switchgrass ball-milled lignin before and after dilute acid pretreatment. Appl Biochem Biotechnol 162:62–74
19. Pingali SV, Urban VS, Heller WT, McGaughey J, O'Neill H, Foston M, Myles DA, Ragauskas A, Evans BR (2010) Breakdown of cell wall nanostructure in dilute acid pretreated biomass. Biomacromolecules 11:2329–2335
20. Pu Y, Hu F, Huang F, Davison BH, Ragauskas AJ (2013) Assessing the molecular structure basis for biomass recalcitrance during dilute acid and hydrothermal pretreatments. Biotechnol Biofuels 6:15
21. DeMartini JD, Pattathil S, Avci U, Szekalski K, Mazumder K, Hahn MG, Wyman CE (2011) Application of monoclonal antibodies to investigate plant cell wall deconstruction for biofuels production. Energy Environ Sci 4:4332–4339
22. Nitsos CK, Matis KA, Triantafyllidis KS (2013) Optimization of hydrothermal pretreatment of lignocellulosic biomass in the bioethanol production process. ChemSusChem 6:110–122
23. Chundawat SPS, Donohoe BS, da Costa Sousa L, Elder T, Agarwal UP, Lu F, Ralph J, Himmel ME, Balan V, Dale BE (2011) Multi-scale visualization and characterization of lignocellulosic plant cell wall deconstruction during thermochemical pretreatment. Energy Environ Sci 4:973–984
24. Alizadeh H, Teymouri F, Gilbert T, Dale BE (2005) Pretreatment of switchgrass by ammonia fiber explosion (AFEX). Appl Biochem Biotechnol 124:1133–1141
25. Rabelo SC, Maciel Filho R, Costa AC (2009) Lime pretreatment of sugarcane bagasse for bioethanol production. Appl Biochem Biotechnol 153:139–150
26. Kawai T, Nakazawa H, Ida N, Okada H, Tani S, Sumitani J, Kawaguchi T, Ogasawara W, Morikawa Y, Kobayashi Y (2012) Analysis of the saccharification capability of high-functional cellulase JN11 for various pretreated biomasses through a comparison with commercially available counterparts. J Ind Microbiol Biotechnol 39:1741–1749
27. Rolando C, Monties B, Lapierre C (1992) Thioacidolysis. In: Lin SY, Dence CW (eds) Methods in lignin chemistry. Springer, Berlin, pp 334–349
28. Fujimoto A, Matsumoto Y, Chang HM, Meshitsuka G (2005) Quantitative evaluation of milling effects on lignin structure during the isolation process of milled wood lignin. J Wood Sci 51:89–91
29. Leschinsky M, Zuckerstätter G, Weber HK, Patt R, Sixta H (2008) Effect of autohydrolysis of *Eucalyptus globulus* wood on lignin structure. Part 2: influence of autohydrolysis intensity. Holzforschung 62:653–658
30. Li J, Henriksson G, Gellerstedt G (2007) Lignin depolymerization/repolymerization and its critical role for delignification of aspen wood by steam explosion. Bioresour Technol 98:3061–3068
31. Dence CW (1992) Determination of lignin. In: Lin SY, Dence CW (eds) Methods in lignin chemistry. Springer, Berlin, pp 33–61
32. Katahira R, Sluiter JB, Schell DJ, Davis MF (2013) Degradation of carbohydrates during dilute sulfuric acid pretreatment can interfere with lignin measurements in solid residues. J Agric Food Chem 61:3286–3292
33. Kanazawa Y, Kishimoto T, Koda K, Fukushima K, Uraki Y (2009) Evaluation of reaction efficiency of thioacidolysis for cleavage of β-*O*-4 interunitary linkages by using β-*O*-4 type artificial lignin polymer. J Wood Chem Technol 29:178–190
34. Awano T, Takabe K, Fujita M (2002) Xylan deposition on secondary wall of *Fagus crenata* fiber. Protoplasma 219:106–115
35. Kim JS, Awano T, Yoshinaga A, Takabe K (2012) Ultrastructure of the innermost surface of differentiating normal and compression wood tracheids as revealed by field emission scanning electron microscopy. Planta 235:1209–1219
36. Jansen S, Smets E, Baas P (1998) Vestures in woody plants: a review. IAWA J 19:347–382